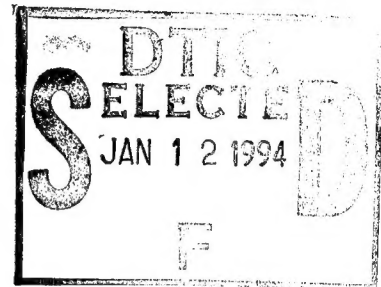


NATIONAL AIR INTELLIGENCE CENTER



STUDY OF FREQUENCY DOUBLING ANTIREFLECTION COATING

by

Wang Mingli, Fan Zhengxiu



19950109 116

DTIC QUALITY INSPECTED 1

Approved for public release;
Distribution unlimited.



HUMAN TRANSLATION

NAIC-ID(RS)T-0102-93

15 December 1994

MICROFICHE NR: 94000560

STUDY OF FREQUENCY DOUBLING ANTIREFLECTION COATING

By: Wang Mingli, Fan Zhengxiu

English pages: 15

Source: Houang Hshu, Vol. 16, Nr. 3, 1992;
pp. 167-172

Country of origin: China

Translated by: SCITRAN
F33657-84-D-0165

Quality Control: Nancy L. Burns

Requester: NAIC/TATD/Bruce Armstrong

Approved for public release; Distribution unlimited.

THIS TRANSLATION IS A RENDITION OF THE ORIGINAL FOREIGN TEXT WITHOUT ANY ANALYTICAL OR EDITORIAL COMMENT STATEMENTS OR THEORIES ADVOCATED OR IMPLIED ARE THOSE OF THE SOURCE AND DO NOT NECESSARILY REFLECT THE POSITION OR OPINION OF THE NATIONAL AIR INTELLIGENCE CENTER.

PREPARED BY:

TRANSLATION SERVICES
NATIONAL AIR INTELLIGENCE CENTER
WPAFB, OHIO

GRAPHICS DISCLAIMER

All figures, graphics, tables, equations, etc. merged into this translation were extracted from the best quality copy available.

Accession For	
NTIS GRA&I	<input checked="" type="checkbox"/>
DTIC TAB	<input type="checkbox"/>
Unannounced	<input type="checkbox"/>
Justification	
By	
Dist. Status	
<div> <div> </div> <div> </div> </div>	
DIC	<div> <div> </div> <div> </div> </div>
A-1	

STOP HERE

ABSTRACT This article carries out detailed study and discussion, both theoretically and in terms of experimentation, on frequency doubling dual wavelength increased transparency or anti-reflection films or coatings. It puts forth film or coating series designs and error analysis, as well as production processes, and solves problems of film or coating uniformity and waveband width.

I. FORWARD

Following along with the development of laser technology, even higher requirements were presented in thin film optics, and frequency doubling dual wavelength increased transparency or anti-reflection thin film coatings are just one among these. Frequency doubling dual wavelength increased transparency films are pointed toward simultaneous increased transparency at $0.53\mu\text{m}$ and $1.06\mu\text{m}$.

The relevant frequency doubling dual wavelength increased transparency film theory and production technology have already been reported a number of times⁽¹⁻⁴⁾. However, starting with the actuality, frequency doubling dual wavelength increased transparency film coatings still possess a number of problems. Take for example, the problem of large base plate uniformity and the problem of waveband width. From theory and experimentation, we have carried out detailed study and discussion, and we have come out with film coating series designs and error analyses as well as production processes. In conjunction with this, we solved the large base plate uniformity problem and the waveband width problem.

II. THEORETICAL FOUNDATION

Considering the various individual parameters associated with multi-layer media increased transparency

systems, one assumes film coating thicknesses to be respectively $d_1, d_2, d_3 \dots$, refraction indices to be respectively, $n_1, n_2, n_3 \dots$, the base to be n_s (1.52), and the incident medium to be $n_0(1)$.

When light rays are vertically incident, the system reflection coefficient is :

$$r = \frac{(M_{11}n_0 - M_{22}n_s) + i(M_{12}n_0n_s - M_{21})}{(n_0M_{11} + M_{22}n_s) + i(M_{12}n_0n_s + M_{21})}$$

In the equation, the matrix elements M_{11}, M_{12}, M_{21} , and M_{22} , are given by the form below:

$$\begin{pmatrix} M_{11} & i M_{12} \\ i M_{21} & i M_{22} \end{pmatrix} = \prod_{j=1}^n \begin{pmatrix} \cos \varphi_j & i/n_j \sin \varphi_j \\ i n_j \sin \varphi_j & \cos \varphi_j \end{pmatrix}$$

$$\varphi_j = \frac{2\pi}{\lambda} n_j d_j$$

In order to satisfy the requirements of zero reflection, it is only necessary that

168

(1)

$$\begin{cases} n_0 M_{11} - n_s M_{22} = 0 \\ n_0 n_s M_{12} - M_{21} = 0 \end{cases}$$

(2)

We opted for the use of multi-layer film coating series which have equal thicknesses. The reason is that they simultaneously satisfy conditions for zero reflection in locations where wavelengths have phase φ . At locations with phases $\pi - \varphi$, they are also capable of satisfying zero reflection. Because this is the case, it is only necessary to consider a wavelength point.

$$\begin{cases} \varphi = \frac{2\pi}{\lambda_1} nd \\ \pi - \varphi = \frac{2\pi}{\lambda_2} nd \end{cases}$$

$$\lambda_2 / \lambda_1 = 1/2$$

$$\varphi = \pi/3$$

(3)

One obtains

Assuming the use of two layer film coating series, one sets up equations (1), (2), and (3) simultaneously and obtains

$$\begin{cases} n_1 = 0.88 \\ n_2 = 1.75 \end{cases}$$

Materials with $n_1=0.88$, in reality, do not exist. In order to facilitate the realization of a selection of refraction index, we make use of three layer film coating systems. We set up equations (1), (2), and (3) simultaneously, and, in conjunction with that, we set $n_1 = 1.46$. The material with 1.46 is SiO_2 . One obtains

$$\begin{cases} n_1 = 1.46 \\ n_2 = 1.67 \\ n_3 = 1.92 \\ nd = 1767 \text{ \AA} \end{cases}$$

On the basis of the results above, we respectively opt for the use of the three material types SiO_2 , Al_2O_3 , and ZrO_2 as matches, and we opt for the use of extreme value methods of control, $\lambda_{\text{control}} = 7068 \text{ \AA}$.

III. ERROR ANALYSIS

As far as the production of multi-layer film coatings is concerned, besides selecting appropriate materials and evaporation techniques in order to guarantee the uniformity of film layer thicknesses, the key problem is overseeing the precision of the thickness of each film layer. If control errors are too large, it is not possible to produce predetermined thin film systems. Error control should guarantee being within a permissible range of deviation.

Our control method is to opt for the use of extreme value control methods. Assuming, when controlling one quarter wavelength, the rate of reflection is an error of ΔR , the corresponding phase error associated with phase φ is φ_A . One opts for the use of excess correction control, that is, $\varphi_1 = \pi/2 + \varphi_A$.

When light rays are vertically incident, the characteristic matrix associated with film thickness (index of refraction is n_A) and base (n_s) is:

$$\begin{bmatrix} B \\ C \end{bmatrix} = \begin{bmatrix} \cos \varphi_1 & i/n_A \sin \varphi_1 \\ i n_A \sin \varphi_1 & \cos \varphi_1 \end{bmatrix} \begin{bmatrix} 1 \\ n_s \end{bmatrix}$$

Due to the fact that $\cos \varphi_1 = -\sin \varphi_A$, $\sin \varphi_1 = \cos \varphi_A$, the aggregate conductance or acceptance is:

$$Y = \frac{C}{B} = \frac{i n_A \cos \varphi_A - n_s \sin \varphi_A}{-\sin \varphi_A + i n_s / n_A \cos \varphi_A}$$

Let

$$\sin \varphi_A \approx \varphi_A, \quad \cos \varphi_A \approx 1 - \varphi_A^2/2$$

169

One then has:

$$Y = \frac{in_A (1 - \frac{1}{2}\varphi_A^2) - n_s \varphi_A}{-\varphi_A + i \frac{n_s}{n_A} (1 - \frac{1}{2}\varphi_A^2)}$$

The index of refraction controlled in a vacuum is:

$$R + \Delta R = r \cdot r^*$$

$$r = \frac{(n_s - 1)\varphi_A + i \left(\frac{n_s}{n_A} - n_A \right) \left(1 - \frac{\varphi_A^2}{2} \right)}{-(1 + n_s)\varphi_A + i \left(\frac{n_s}{n_A} + n_A \right) \left(1 - \frac{\varphi_A^2}{2} \right)}$$

Then

$$R + \Delta R = \frac{(n_s - 1)^2 \varphi_A^2 + \left(\frac{n_s}{n_A} - n_A \right)^2 \left(1 - \frac{\varphi_A^2}{2} \right)^2}{(n_s + 1)^2 \varphi_A^2 + \left(\frac{n_s}{n_A} + n_A \right)^2 \left(1 - \frac{\varphi_A^2}{2} \right)^2}$$

$$= \left(\frac{n_s/n_A - n_A}{n_s/n_A + n_A} \right)^2 \left(1 + \frac{\left(n_s^2 + 1 - n_A^2 - \frac{n_s^2}{n_A^2} \right) 4n_s}{(n_s^2/n_A^2 - n_A^2)^2} \varphi_A^2 \right) \quad (4)$$

Due to the fact that there is no error when

$$R = \left(\frac{n_s/n_A - n_A}{n_s/n_A + n_A} \right)^2 \quad (5)$$

Comparing equations (4) and (5), one obtains

$$\Delta R = \frac{\left(n_s^2 + 1 - n_A^2 - \frac{n_s^2}{n_A^2} \right) 4n_s}{(n_s^2/n_A^2 - n_A^2)^2} \varphi_A^2 \quad (6)$$

The expression for ΔR which is arrived at here and the one reported by H.A.Madeod in reference (5)

$$\Delta R = \frac{4n_s(n_A^2 - 1) \left(1 - \frac{n_s^2}{n_A^2}\right)}{(1 + n_s)^4} \varphi_A^2$$

They are different in places. This is due to the fact that Madeod, in deducing his expression for ΔR , did not consider the phase thickness of thin films themselves (when there is no error). He only considered phase thickness associated with errors.

Let

$$\text{令: } M = \frac{(n_s^2 + 1 - n_A^2 - n_s^2/n_A^2)4n_s}{(n_s^2/n_A^2 - n_A^2)^2}$$

Therefore

$$\text{所以 } \varphi_A = \sqrt{\frac{\Delta R}{M}} \quad (7)$$

Due to errors associated with the index of refraction ΔR for the 1st layer, this leads to phase thickness error φ_A . Therefore, this also makes the 2d layer induce a phase thickness error φ_B , as is shown in Fig.1. Consider the fact that the admittance loci associated with nonabsorptive films form a clockwise circular track on complex admittance planes.

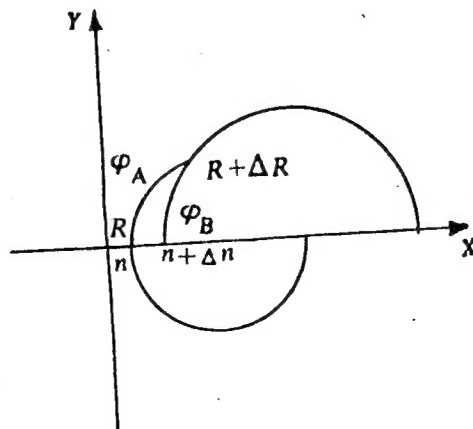


Fig.1 Phase Thickness Errors Associated with Film Layers A

From Fig.1 it is possible to see that the phase error for layer A is $\pi/2 + \varphi_A$. Due to the existence of error φ_B , the intersection point between film layer B and the real axis changes from n to $n + \Delta n$,

170

$$\begin{pmatrix} B \\ C \end{pmatrix} = \begin{pmatrix} \cos \varphi_B & \frac{i}{n_B} \sin \varphi_B \\ i n_B \sin \varphi_B & \cos \varphi_B \end{pmatrix} \cdot \begin{pmatrix} \cos \left(\frac{\pi}{2} + \varphi_A \right) & \frac{i}{n_A} \sin \left(\frac{\pi}{2} + \varphi_A \right) \\ i n_A \sin \left(\frac{\pi}{2} + \varphi_A \right) & \cos \left(\frac{\pi}{2} + \varphi_A \right) \end{pmatrix} \cdot \begin{pmatrix} 1 \\ n_s \end{pmatrix}$$

As far as the aggregate admittance $Y=C/B$ is concerned, in order to solve for $n + \Delta n$, one makes the imaginary part of $Y=C/B$ equal to zero, eliminating φ_A and φ_B 's higher order terms to obtain

$$\varphi_B = - \frac{n_A - n_s^2/n_A}{n_A^2/n_B - n_B \cdot n_s^2/n_A^2} \varphi_A \quad (8)$$

The result derived here and the one derived by H.A.Macleod in reference (5)

$$\varphi_B = - \frac{n_A - n_s^2/n_A}{n_B - n_s^2/n_B} \varphi_A$$

are also different in places. In the same way, this is due to Macleod's ignoring the phase thickness of the 1st film layer (that is, film layer A) itself.

$$\text{Make:} \quad N = - \frac{n_A - n_s^2/n_A}{n_A^2/n_B - n_B \cdot n_s^2/n_A^2} \quad (9)$$

In these equations, φ_A and φ_B are reciprocal symbols. If the 1st layer has a positive error, then, in

that case, the excess positive or excess correction of the 1st layer is just right for the use of inadequate φ_B compensation associated with the second layer. In the same way, the 2d layer, in the process of evaporation, shows the existence of control error ΔR_B . In this way, the complete error associated with the 2d layer film should include two parts, that is

$$N_1 \varphi_A + \sqrt{\frac{\Delta R_B}{|M_2|}}.$$

By the same principles, we are capable of obtaining the 3d layer error

$$N_2 \varphi_B + \sqrt{\frac{\Delta R_C}{|M_3|}}.$$

In this, N_1 , N_2 , M_2 , and M_3 are obtained, respectively, on the basis of equivalent film layers.

During actual supervisory control, refractive index control errors are, generally, composed of two terms, that is, the error α when a head passes the location of a value turning point and the random signal error β . In normal situations, α and β approximate normal distributions, within permitted ranges, giving the head pass error α and the random error β associated with refractive index control errors for each layer of film. Following this, from the normal functions P_1 , P_2 for two (0,1) distributions produced by computer, it is possible to display the reflective index errors as: $\Delta R = P_1 \alpha + P_2 \beta$. Assuming α is 1.0% and β is 0.5%^(6,10),

From the derivations above, it is possible to obtain 1st layer error:

$$\varphi_A = 0.1036, \quad P_{R1} = \frac{\varphi_A}{\pi/2} = 6.6\%.$$

2d layer error:

$$\varphi_B = -0.0509, \quad R_{R2} = \frac{\varphi_B}{\pi/2} = -3\%.$$

3d layer error:

$$\varphi_c = 0.1708, \quad P_{\text{c}} = \frac{\varphi_c}{\pi/2} = 10.8\%.$$

When errors of 6.6%, -3%, and 10.8%, respectively, exist in three layer film thicknesses, the three layer film thicknesses are, respectively:

$$\begin{array}{ll} n_1 = 1.92, & 1883 \text{ \AA}, \\ n_2 = 1.67, & 1714 \text{ \AA}, \\ n_3 = 1.46, & 1957 \text{ \AA}, \end{array}$$

Using numerical data for the three film thicknesses above and entering it into a computer, one obtains the results below:

171

$$\begin{array}{lll} \text{where } & 0.53 \mu\text{m} & R = 0.0008 \\ \text{where } & 1.06 \mu\text{m} & R = 0.0005 \end{array}$$

The computer programs were supplied by Shanghai Optical Instruments Institute. The results above clearly show that using extreme value methods controls errors within permissible ranges.

IV. PRODUCTION TECHNIQUES

1. Characteristics of ZrO_2 Film Material

ZrO_2 material is a block material which is sintered or agglomerated for 2 hours in a 1200°C high temperature furnace, using an E type electron gun for evaporation or volatilization. The magnitudes of ZrO_2 film refractive indices and basic temperatures as well as degrees of vacuum and speed of sedimentation are very greatly dependent on

each other. In this way, giving the illuviation or deposition brings the greatest difficulties. Therefore, fixing evaporation or volatilization conditions is an extremely important question. Moreover, the basic temperatures and degrees of vacuum associated with evaporation or volatilization conditions can be maintained invariable. In this way, the key question is none other than evaporation or volatilization speeds. Control of evaporation or volatilization speeds depends on the degree of familiarization of the operating personnel and technical levels. Since evaporation or volatilization speeds cannot be too fast, they also cannot be too slow. Too fast, and it is easy to form large granular crystals, making the thin film surfaces turn very coarse. Too slow, and refractive indices are not able to reach requirements. Moreover, this will influence the close and compact nature of thin films.

$v(\text{\AA}/s)$	5	8	10	12	15	40
n	1.821	1.880	1.915	1.925	1.927	2.010

Table 1 Relationship Between Refractive Index n and Evaporation or Volatilization Speed v

Table 1 is experimental results for ZrO_2 refractive indices with different speeds of evaporation or volatilization. The base temperature is 180°C . The degree of vacuum is $1.5 \times 10^{-2} \text{Pa}$.

The data above are average values from multiple iterations of experiments. They speak to single layer films of $\lambda/4$ ($\lambda = 1.06 \mu\text{m}$). They were measured in air. The data above clearly show that refractive indices associated with ZrO_2 material, for given temperatures and air pressures, are very greatly influenced by evaporation or volatilization speeds. Generally speaking, taking 12 \AA/s as a speed of evaporization or volatilization is relatively appropriate.

2. Characteristics of Al_2O_3 Film Material

Al_2O_3 material is a transparent crystal. Its refractive index and evaporation or volatilization conditions are also very greatly related. Under conditions of bad vacuum and low base temperatures, refractive indices are capable of being smaller than 1.52. Under conditions of good vacuum, high base temperatures, and rapid speeds of evaporation or volatilization, they are capable of reaching 1.70. Fig.2 is refractive indices associated with Al_2O_3 for different speeds of evaporation or volatilization. The base temperature is the same 180°C . Degree of vacuum is $1.5 \times 10^{-2} \text{ Pa}$.

$v(\text{\AA/s})$	5	8	10	12	15	18
n	1.551	1.557	1.561	1.612	1.631	1.654

Table 2 Relationships Between Refractive Index n and Speed of Evaporation or Volatilization v

3. Characteristics of SiO₂ Film Material

Large amounts of experimentation verify that the reproducibility of refractive indices for SiO₂ in air is relatively good. Speeds of evaporation or volatilization are relatively fast⁽⁷⁾, and generally 40 Å/s. Due to these characteristics, it is required, when evaporating SiO₂, to pay particular attention to precision control.

V. EXPERIMENTATION

In the process of experimentation, we discovered a number of problems. One is the relative narrowness of wavebands at 0.53 μm locations. This creates difficulties in production work. The second is the relatively bad uniformity of large base plates. Sometimes plate diameters are as large as ϕ 300mm. Large base plate uniformities, besides being related to plating film machine geometrical parameters, are also related to control precision associated with surface configurations at different locations on large plates and base temperature inconsistency causing base layer film thicknesses to be unable to achieve uniformity.

In order to solve the above problems, on the bottom layer, another layer of low refractive index film with $\lambda/2$ (1.06 μm) is added, that is, an SiO₂ film layer. In this way, it is possible to widen the bandwidth at 0.53 μm locations, raising the uniformity of film coating plates⁽¹¹⁾. Thin film nonuniformities of $\pm 1\%$ or more are improved to less than $\pm 0.5\%$. Film thickness uniformity achieves very great advances.

Bottom layer film thickness is $\lambda/2$ (1.06 μm is just one half of a wavelength at 0.53 μm locations, and, at the

same time, just $3/4$ times the control wavelength). Extreme value method control goes for three rounds.

Fig.2 is the theoretical curves with and without the plating of an additional SiO_2 base layer. From the curves of Fig.2, it is possible to see that the waveband widths at $0.53\mu\text{m}$ locations after base layer addition and $1.06\mu\text{m}$ locations are all widened. This facilitates production work. At the same time, there are experiments which clearly show that SiO_2 film laser light loss threshold values basically have no film thickness effects⁽⁹⁾ on thickness dependence relationships. There are also experiments which clearly show that, in increased transparency or antireflection film base layers with the additional plating of SiO_2 , it is possible to raise thin film laser loss threshold values^(8,9).

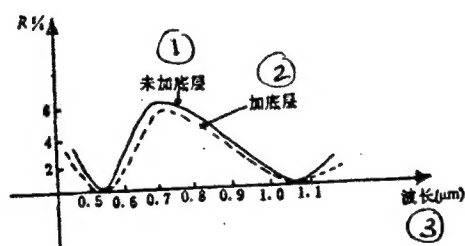


Fig.2 Theoretical Curves With and Without the Additional Plating of SiO_2 (1) Unplated Base Layer (2) Plated Base Layer (3) Wavelength

Table 3. Experiment Results

	R	
	0.53(μm)	1.06(μm)
1	1‰	1‰
2	1.5‰	1.5‰
3	0.5‰	1‰
4	1‰	2‰
5	1‰	0.5‰

Table 3 is the latest experimental results. From the results, one can see that experimental results and theoretical numerical values agree. What is worth drawing attention to is the fact that the refractive index associated with Al_2O_3 will be lower compared to the refractive index associated with theoretical designs. Therefore, when plating Al_2O_3 , one should exert every effort to enlarge the refractive index.

We express our thanks to Comrades Li Qingguo, Fan Ruiying, and Wu Zhouling, who presented their valuable points of view on this work.

REFERENCES

- [1] Mouchat J. Appl Opt, 1977; 16 (9) : 2486
- [2] Mouchat J. Appl Opt, 1977; 16 (11) : 3001
- [3] Nagendra C. Appl Opt, 1988; 27 (11) : 2320
- (4) Li Qingguo; China Laser, 1984, 11(2): 114
- [5] Macleod H A. Opt Acta, 1972; 19 (1) : 1~28
- (6) Tang Pufa; Thin Film Optics, Shanghai: Shanghai Scientific and Technical Press, 1984

- (7) Fan Ruiying; LF12 Test Production Work Report, 1987
- (8) Fan Zhengxiu; China Laser, 1982; 9(9): 582
- (9) Wu Zhouling; Doctoral Thesis; Shanghai Optical Instruments Institute, 1988: 91
- (10) Li Li; Doctoral Thesis; Shanghai Technical Physics Institute; 1987: 31
- (11) Tan Shusheng; Optics Journal, 1984; 4(4): 355

A Brief Introduction to the Author: Wang Mingli. Male.
Born May 1965. Assistant Engineer. At present, engaged in
research work on thin optical films.

DISTRIBUTION LIST

DISTRIBUTION DIRECT TO RECIPIENT

<u>ORGANIZATION</u>	<u>MICROFICHE</u>
B085 DIA/RTS-2FI	1
C509 BALLOC509 BALLISTIC RES LAB	1
C510 R&T LABS/AVEADCOM	1
C513 ARRADCOM	1
C535 AVRADCOM/TSARCOM	1
C539 TRASANA	1
Q592 FSTC	4
Q619 MSIC REDSTONE	1
Q008 NTIC	1
Q043 AFMIC-IS	1
E051 HQ USAF/INET	1
E404 AEDC/DOF	1
E408 AFWL	1
E410 AFDTC/IN	1
E429 SD/IND	1
P005 DOE/ISA/DDI	1
P050 CIA/OCR/ADD/SD	2
1051 AFTT/LDE	1
PO90 NSA/CDB	1
2206 FSL	1

Microfiche Nbr: FTD94C000560
NAIC-ID(RS)T-0102-93